Proceedings World Geothermal Congress 2005
Antalya, Turkey, 24-29 April 2005

Flashing Phenomena in the Case of Two-Phase Flow (Liquid-Gas) in a Vertical Porous Channel

C. Seladji [(1)] S,R Taleb [(2)], Y. Khadraoui [(1)]

[(1)] Université Abou Bakr BELKAID, Tlemcen 13000, Algeria

Email : Seladji@yahoo.fr

[(2)] Ecole de Technologie supérieure , Université du Quebec, Montréal Canada

Email : Staleb@mec.etsmtl.ca

Keywords: Two-phase flows- porous media- capillary pressure- relative permeability -flashing- separate flow model.

ABSTRACT

In this paper, flashing phenomena are studied in the case of water-steam and air outflow in a vertical porous channel . The presence of air, the nature of the porous environment, as well as injected fluid thermo-physics parameters are analyzed.

The separate flow model approach which takes the individual properties of air and water separately is considered. On the other hand, we consider that water and its steam are represented as a mixture characterized by the mean properties according to the quality (x)(the ratio of the vapor mass and the total mass).

Some results show that the porous environment as well as the presence of air represent a resistance to the water outflow. When the effective permeability (or the relative permeability) decreases, the pressure of injection of water increases to maintain the same flow rate. In this case, a decrease of steam generated is observed.

1. INTRODUCTION

Multi-phase flows in porous media are phenomena currently met in different industrial fields. Examples include geothermal systems, oil reservoir engineering, post accident analysis of nuclear reactors, drying processes and thermal energy storage. These phenomena were the object of a multitude of applied studies as well as numerous attempts of mathematical modeling.

The flashing phenomena are met in several cases. Indeed, oil extraction is bound to the creation of associated gases. These dissolved gases intervene when the liquid phase reaches saturation conditions. We can also mention the example of the sea water desalination technologies for producing drinking water, which use a multi-flashing process.

Several studies have been led in order to solve problems bound to this kind of flow while adopting some classical multi-component mixture models Bowen (1976) of two or several constituents, considering the average thermo-physical properties of the fluids. A two-phase mixture approach developed by Wang and Beckermann (1993), built from a separate flow model introduces capillary effects in its linear formulation (Darcy's flow). The conservation equations are derived from the separate flow model without invoking additionnal assumptions. The separate flow model (SFM) as discussed by Scheidegger (1974) or Bear (1972), which uses every phase characteristics separately, taking into account the interactions between the fluids (the capillary pressure and the relative permeability) is considered as a more rigorous approach, but represents some difficulties to be solved.

2. TWO-PHASE FLOW MODELS

Carbonell and Whitaker (1982); Whitaker (1969) developed some models resulting from the average of the microscopic equations (continuity and momentum). Sàez (1984) discussed in detail the macroscopic equations of motion governing two-phase flow in packed beds in the isothermal non-reaction conditions. The generalized Darcy's two-phase flow equations, which include the microscopic and macroscopic inertial terms mentioned by Grosser and Al. (1988), introduce the microscopic inertial coefficients CF_i for the two-phase flow as follows:

$$CF_i = \frac{K^{1/2}}{C_E} CF_{ri} \tag{1}$$

K is the permeability of the porous media, C_E is the Eurgun constant and CF_{ri} is a relative inertial permeability. These coefficients account for the entire excess pressure drop due to the phase velocities which are relatively large. The factors influencing the microscopic inertial coefficients are the same as those that influence the phase permeabilities.

Saez and Carbonnell (1985) proposed the following correlation to describe the CF_{ri}

$$\begin{cases} CF_{rl} = K_{rl} \\ CF_{rg} = K_{rg} \end{cases} \tag{2}$$

K_{rl} K_{rg} are the relative permeabilities which are given in Table 1.

Schulenberg and Müller (1987) propose the following correlations:

$$\begin{cases} CF_{rl} = S^5 & 0 \le S \le 0.7 \\ CF_{rg} = (1-S)^6 & 0 \le S \le 0.7 \\ CF_{rg} = 0.1(1-S)^4 & 0.7 \le S \le 1 \end{cases} \tag{3}$$

2.1 The relative permeability model

The concept of relative permeability K_r has been used for each phase by Sàez and Carbonell (1985). The effective permeability is given by K_i :

$$K_i = K.K_{ri} \tag{4}$$

Where K is the porous medium permeability and K_{ri} the relative permeability for each phase. Marle (1981) has established that the relative permeabilities are functions of several parameters involving the properties of both the fluid and the medium. Usually, it is assumed that K_r depends essentially on the phase saturation S . Several studies were conducted to establish the relationships between the relative permeabilities and the saturation. The most commonly used relationships as mentioned by M. Fourar and Lenormand (2000) are power law functions e.g. Corey (1954) :

$$K_{rl} = S_e^4 \tag{5}$$

$$K_{rg} = (1-S_e)^2(1-S_e^2) \tag{6}$$

In these relations, S_e is the effective liquid phase saturation defined by :

$$S_e = \frac{S_l - S_r}{1-S_r} \tag{7}$$

Where S_l is the liquid saturation and S_r the residual saturation. In fact, the value of the exponent in equations (5) and (6) has been found to vary for different porous media as given by Brooks and Corey (1966). Some relationships established by Buckley and Levrett (1942) reported by Houpert (1974) , and based on Corey works are used :

$$K_{rl} = \left(\frac{0.8 - s_g}{0.8}\right)^4 \tag{8}$$

$$K_{rg} = \frac{25}{9}\cdot(s_g - 0.2)^2 \quad , \quad 0.2 \le s_g \le 0.65 \tag{9}$$

$$K_{rg} = 1 - \frac{25}{7}\cdot(s_g - 1)^2 \quad , \quad 0.65 \le s_g \le 1 \tag{10}$$

S_g is the gas saturation

The main correlations defining K_{rl} and K_{rg} and found in the literature for porous media are given in Table 1. S_e is the effective saturation defined by the relation (7) .

Table 1: Correlations for relative permeabilities

	K_{rl}	K_{rg}
Lipinski (1980)	S_l^3	1-1.11 S_l
Lipinski (1982)	S_l^3	$(1- S_l)^3$
Turland and Moore (1983)	S_l^3	1- S_l
Schulenberg and Müller (1984)	S_e^3	$(1- S_e)^3$
Saez and Carbonnell (1985)	$S_e^{2.13}$	$(1- S_e)^{1.8}$

Some studies given by Horne and al (2000) have conducted steam-water relative permeabilities experiments. However, the fact that the water and its steam can easily change from one to the other, generate some difficulties. Globally, they conclude that steam-water relative permeabilities in a porous rock follow the Corey-type behavior.

2.2 The Capillary pressure model

The capillary pressure model given by scheidegger (1974) is defined as the volume average pressure difference between the gas phase and the liquid phase in a porous medium.

$$P^g - P^l = P_c(s) \tag{11}$$

This pressure difference is the result of the surface tension forces that depend on the average curvature of the gas-liquid interfaces. Levrett (1941) developed a correlation for capillary pressures in packed beds of unconsolidated materials:

$$P_c = \sigma\sqrt{\frac{\varepsilon}{k}}J(S_l) \tag{12}$$

$J(S_l)$ is the Levrett function. It depends only on the liquid saturation. Other correlations are obtained from experiments. These correlations are drawn from either the imbibition or the drainage experimental data. Using Levrett experiments, Scheiddeger (1974) proposed for water-air two-phase flow in sand :

$$P_c = \frac{\sigma}{(k/\varepsilon)^{1/2}}\cdot\left[\begin{matrix}0.364\cdot\left(1-e^{-40.(S_g)}\right)+0.221\cdot S_g \\ +\dfrac{0.005}{0.96-S_g}\end{matrix}\right] \tag{13}$$

σ is the surface tension between phases, S_g is the saturation of the gas phase, ε is the porosity of the porous environment and K is the medium permeability .

2.3 The energy balance description

The energy equations for two phase flow in porous media result from local volume averaging of the conservative energy equation. This concept has been developed by Whitaker (1977). The convection-diffusion energy equations for each phase are given as follows: (i : solid, liquid and gas phases)

$$(\rho c)_i\left(\frac{\partial T_i}{\partial t} + \vec{v}.\nabla T_i\right) = k_i.\nabla^2 T_i + u_i''' \tag{14}$$

The local volume averaging treatment is applied. The derivation details are given by Whitaker (1977) .

The concept of the effective thermal conductivity is introduced. It is considered as the combination of the liquid, the solid and the gas contributions to the molecular conduction. The thermal dispersion is the combined dispersion in the liquid and the gas phases.

In fact, the convection-diffusion energy equations are given from more general equation. The variation of internal energy according to the first principle of thermodynamics, corresponds respectively to the sum of the reversible compression effects, the thermal diffusion term, the heat energy generation and the irreversible viscous dissipation effects. For each phase (liquid, solid and gas), we have the following equation :

$$\frac{d(\rho_i \cdot U_i)}{dt} = -P_i\nabla\vec{v_i} + \nabla(k_i.\nabla T_i) + u_i''' + \mu_i\phi \tag{15}$$

where

$$dU_i = dh_i - d\left[\frac{P_i}{\rho_i}\right] \quad (16)$$

U_i , h_i , P_i and ρ_i are respectively the internal energy, the enthalpy, the pressure and the density of each phase.

For the liquid phase, which is concerned by the flashing phenomena, we disregard the heat transfer term (isentropic), the heat energy generation term as well as the irreversible viscous dissipation effects. We consider only the reversible compression effects in a steady state case. Thus, equation (15) can be rewritten using equation (16) as :

$$\nabla(\overline{\rho}_l \cdot \overline{h}_l \vec{\overline{v}}_l) = \nabla(\overline{P}_l \cdot \vec{\overline{v}}_l) \quad (17)$$

$\overline{U}_l$, $\overline{h}_l$, $\overline{P}_l$ and $\overline{\rho}_l$ are the average characteristics of the liquid mixture (water + steam). Equation (17) written in a microscopic scale is used for the local volume averaging treatment. As given by Whitaker (1977), this technique takes into account a deviation from the average values as follows:

$$\begin{cases} \overline{h}_l = \langle \overline{h}_l \rangle + \overline{h}_l^* \\ \vec{\overline{v}}_l = \langle \vec{\overline{v}}_l \rangle + \vec{\overline{v}}_l^* \\ \overline{P}_l = \langle \overline{P}_l \rangle + \overline{P}_l^* \end{cases} \quad (18)$$

$$\langle \nabla(\overline{\rho}_l \cdot \overline{h}_l \vec{\overline{v}}_l) \rangle = \langle \nabla(\overline{P}_l \cdot \vec{\overline{v}}_l) \rangle \quad (19)$$

Using Equation (18), Equation (19) becomes :

$$\varepsilon.S_l \nabla\left[\langle \overline{\rho}.\overline{h} \rangle^l \cdot \langle \vec{\overline{v}} \rangle^l\right] = \varepsilon.S_l \nabla\left[\left(\langle \overline{P}^* \rangle^l - \langle \overline{\rho}.\overline{h}^* \rangle^l\right)\langle \vec{\overline{v}}^* \rangle^l\right] + \varepsilon.S_l\left[\langle \overline{P} \rangle^l . \langle \vec{\overline{v}} \rangle^l\right] + \int_A \left(\overline{P} - \overline{\rho}.\overline{h}\right) \vec{\overline{v}}_l \, dA \quad (20)$$

The averaging method reveals the dispersion flux owed to local variations of the velocity and the enthalpy. It reveals also a transfer through the mixture interface. This equation will be used further.

The flashing phenomena are bound to the pressure drop, which is considered the unique source of energy provoking the evaporation in our case (isentropic). Lackmé (1980) proposed to introduce an indicator of spraying *(y)*. This indicator represents the mass fraction of metastable liquid that turned on, into steam, and in liquid, which becomes in thermal equilibrium with this steam. It begins to have a physical significance at the section where the boiling point *(P_0)* appears. The determination of this pressure requires a good knowledge of nucleation conditions. Lackmé supposed that the beginning of the spraying pressure is proportional to the pressure of saturation *(P_{sat})* corresponding to the temperature of entry.

$$P_0 = \Omega_1 . P_{sat}(T_e) \qquad \Omega_1 = 0.95 \ldots 0.97 \quad (21)$$

Hardy and Mali (1982) proposed that this indicator Ω_1 is a function of some experimental parameters.

3. MATHEMATICAL FORMULATION

3.1 Assumptions

The problem has been solved using a steady state. Fluids (air and water) are supposed incompressible. We assume that the local thermal equilibrium exists among the three phases (liquid, solid and gas).

We consider that there is no mass absorbed in interfaces and no heat energy transferred to the mixture (liquid + vapor). The energy of evaporation is supposed to come from the liquid pressure drop. The factor of spraying as given by Lackmé (1980) is considered as equal to 1.

As given by Lackmé (1980), the boiling point of the liquid is at $P_0 < P_{sat}(T_{entry})$ corresponding to the temperature at the entry side.

3.2 Momentum Equations

For *i* = air, mixture (water + steam)

$$\frac{\rho_i}{\varepsilon.s_i} \cdot \left(\vec{v}_i . \nabla \vec{v}_i\right) = -\nabla P^i + \rho_i \cdot \vec{g} - \frac{\mu_i}{K_i} \cdot \vec{v}_i + \frac{\mu_i}{\varepsilon.s_i} \nabla^2 \vec{v}_i - \frac{\rho_i}{CF_i} \cdot \left|\vec{v}_i\right| \cdot \vec{v}_i \quad (22)$$

Equation (22) takes into account the microscopic and macroscopic inertial terms.

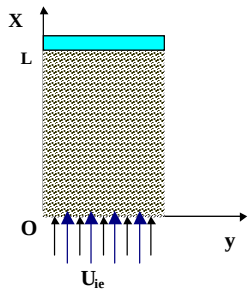

Figure1. Two-phase flow experiments

3.3 Continuity equations

$$\nabla(\overline{\rho}_i \cdot \vec{\overline{v}}_i) = 0 \quad (23)$$

3.4 Closure Equations

$$P^g - \overline{P}^l = P_c(s) \quad (24)$$

$$S_g + S_l = 1 \quad (25)$$

3.5 Energy Equation for the liquid phase

The liquid phase energy equation which is of our interest (Eq. 17) is treated in a representative elementary volume, taking into account the relation between the real velocity and Darcy's velocity:

$$\vec{\overline{v}}_l = \varepsilon.S_l \langle \vec{\overline{v}} \rangle^l \quad (26)$$

Disregarding the dispersion terms due to local variation of pressure and velocity, and considering that there is no existing transfer between interfaces of different phases, equation (20) becomes :

$$\nabla\left[\left(\overline{\rho}\cdot\overline{h}\right)^{l}\cdot\vec{\overline{v}}_{l}\right]=\nabla\left[\overline{P}^{l}\cdot\vec{\overline{v}}_{l}\right] \qquad (27)$$

3.6 Liquid mixture properties

As we have said above, the liquid phase and its steam are considered as a mixture having average properties. In fact, we predict a weak amount of steam generated by flashing. These mixture properties will be calculated according to ρ_l , μ_l , ρ_v , μ_v and x, which are respectively the liquid density and viscosity, the steam density and viscosity and the quality which is defined as the ratio of the vapor mass to the mixture mass.

3.6.1 The mixture density :

$$\overline{\rho}_l=\frac{\rho_l\cdot\rho_v}{(1-x)\cdot\rho_v+x\cdot\rho_l} \qquad (28)$$

The choice of this expression is justified if we admit that the density is an extensive property, but we cannot say as much for the viscosity.

3.6.2 The mixture viscosity

Taking into consideration that the vapor occupies more area than an equivalent mass of liquid , we can use the following relation :

$$\overline{\mu}_l=\frac{(1-x)\cdot\rho_v\cdot\mu_l+x\cdot\rho_l\cdot\mu_v}{\rho_v-x\cdot(\rho_v-\rho_l)} \qquad (29)$$

3.6.3 The mixture Enthalpy

The average enthalpy of the mixture (water+steam) is defined as :

$$\bar{h}=h_l+x.(h_v-h_l) \qquad (30)$$

$(h_l,- h_v)$ is the latent heat of vaporisation at the prevailing pressure. The data of steam-water proprieties is introduced in the calculation code.

3.7 Boundary Conditions

3.7.1 Conditions on velocities

Let's consider $\vec{v}$ (u, v) in a Cartesian reference. U_{ie} is the velocity imposed at the entry. *xp* and *yp* are the coordinates.

for ($i = l, g$)

$$\begin{cases} u_i\,(xp, yp=0)=0 \quad , \quad v_i\,(xp, yp=0)=0 \\ u_i\,(xp, yp=d)=0 \quad , \quad v_i\,(xp, yp=d)=0 \\ u_i\,(xp=0, yp)=U_{ie} \quad , \quad v_i\,(xp=0, yp)=0 \\ \left.\dfrac{\partial u_i}{\partial xp}\right|_{x=L}=0 \quad , \; v_i(xp=L, yp)=0 \end{cases} \qquad (31)$$

3.7.2 Condition on the enthalpy

$$h(xp=0, yp)=h\,(T_0, P_{entry}) \qquad (32)$$

The temperature T_0 is imposed in the entry side.

3.7.3 Conditions on the air saturation

In order to have some known conditions reigning at the exit side (at the top) of the porous massif, we consider that this area remains wet all along the experiment. This assumption permits to consider a critical air saturation S_{gc} *=0.2* e.g. Houpert (1974)

4. METHOD OF RESOLUTION

The problem will be solved using the numerical finite volume method. The SIMPLE algorithm (Semi Implicit Method for Liking Equation) developed by Patankar (1980) is used for the calculation of pressure fields. The saturation S will be known while identifying the pressure difference $P^g - \overline{P}^l$ to the capillary pressure model $P_c(s)$. The Scheidegger model represented by equation (13) is used. The calculation of the liquid pressure $\overline{P}^l$ allows us to know the enthalpy value. The quality x is than deduced.

5 - RESULTS AND INTERPRETATIONS

The generation of the necessary pressure making the liquid to flow, depends on the injected flow rate and the effective permeability which includes the presence of another phase. It depends also on the length of the porous channel. All these parameters represent a resistance which is necessary to compensate.

5.1 A test case (Hassler's experiments)

In order to compare two-phase flow results with some analytical results given by Houpert (1974), we used the relation (8), (9) and (10) to define the relative permeability model and the following relation for the capillary pressure P_C (mbar), ε =0.2, K= 2.10^{-13} m²:

$$P_c=\frac{6400}{0.8-s_g} \qquad (33)$$

Some results corresponding to Hassler's experiments (1944) are given in the goal of validating our calculation code. These experiments consist in injecting a non-wet phase (air) from the bottom to the top. The top extremity is maintained wet. The porous matrix is saturated in wet phase (water) .

Figure 2 represents saturation profiles for different air mass flow rates. From figure 3, we can note that it is necessary to exert an increasing air injection pressure in order to obtain an increasing flow rate. In this case, the air saturation S_g increases (Figure 2).

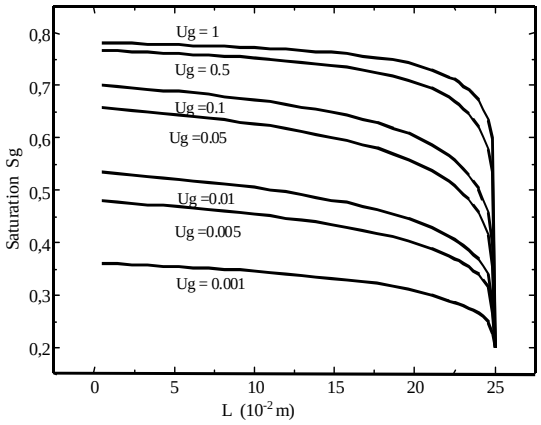

Figure 2. Evolution of air saturation S_g. (u_g : cm/s) (K = 2.10^{-13} m)

This implies an increasing capillary pressure. Identical results are given for an analytical solution of Darcy's linear

equations for one-dimensional problems as given by Houpert (1974).

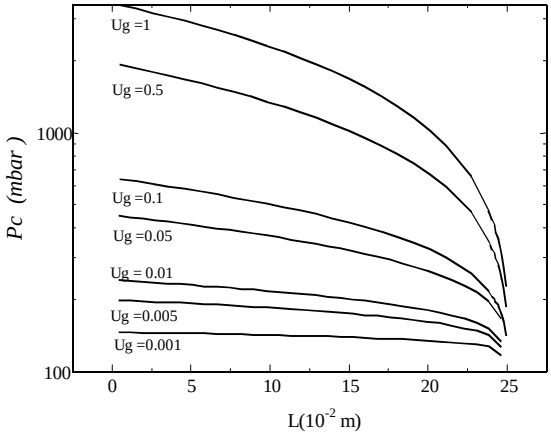

Figure 3. Evolution of the capillary pressure. (u_g : cm/s) (K = 2.10^{-13} m²)

5.2 Analysis of the liquid single-phase flow

In this section, flashing phenomena results are shown for a single-phase flow case, in order to be able to compare with two-phase flow. The liquid is considered at the temperature T = 170°C. The evaporation pressure corresponding to this temperature is P_{sat}= 8,076 bar (properties of water steam). The liquid state at the entry side is given by calculating the injection pressure resulting from momentum equations. In all cases, the water is in sub-cooled or saturated state.

Figure (4) shows that the injection pressure is proportional to the length of the channel. Increasing the channel length leads to a reduction in the generated steam: figure (5). It is obvious that the conditions of the critical out-flow are far from being reached. The liquid velocities in the porous matrix are about 10^{-6} m/s to 5.10^{-3} m/s. It is important to note that the relative length of the mixture flow increases for a decreasing porous channel length.

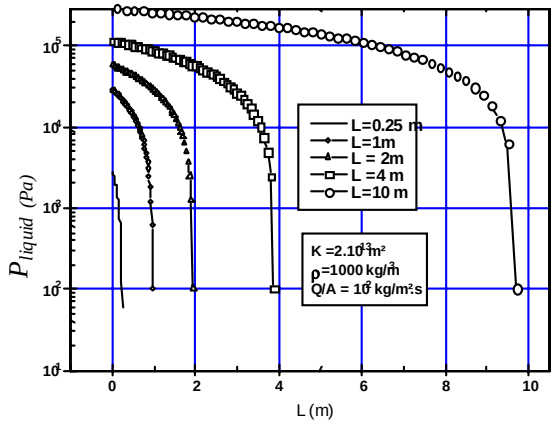

Figure4. Influence of the channel length on the liquid pressure injection

Figure (6) shows that when increasing the water mass flow rate, it becomes necessary to increase the pressure of injection in order to maintain the imposed flow rate. In this case, the pressure of saturation P_{sat} is reached solely at the exit of the channel, where the quality x is reduced .

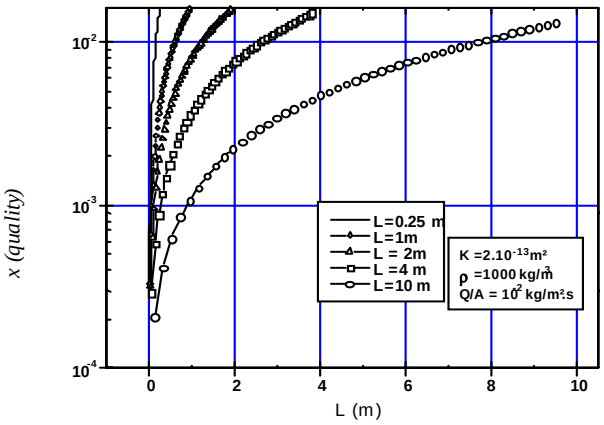

Figure 5. Influence of the channel length on the quality

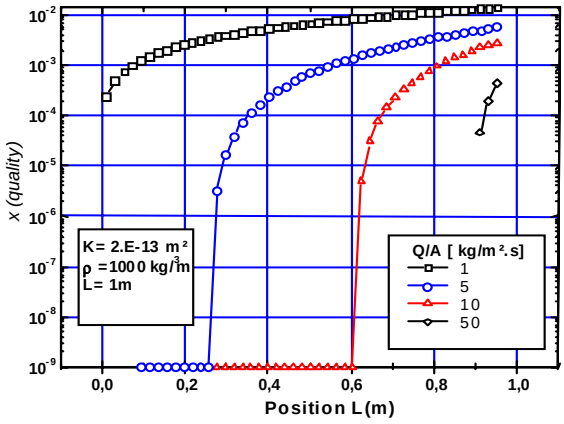

Figure 6. Influence of the injected water mass flow rate on quality

5.3 Analysis of the air/liquid two-phase flow

Contrary to Hassler's experiments, the liquid and the air are injected simultaneously in the porous channel. We consider that the liquid and air are at T=170 °C, being able to reach evaporation conditions inside the porous channel.

Figure (7) shows that the quality x decreases if we compare it with a single-phase flow for the same liquid conditions. We can explain this result by the reduction of the effective permeability facing the water flow. In fact, the relative permeability, which is function of air saturation, decreases. The liquid must generate more injection pressure. The flashing phenomena are delayed and imposed by evaporation conditions met toward the exit side: figure (8).

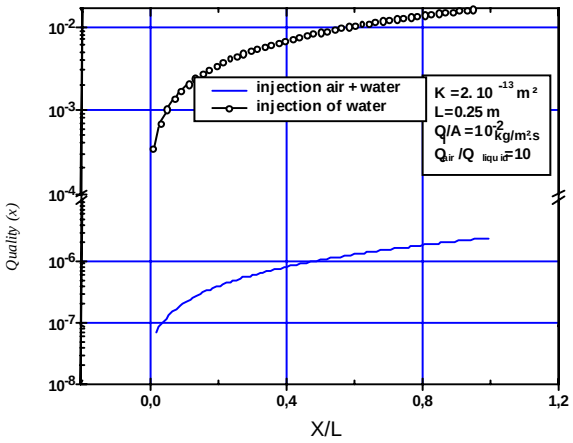

Figure7. Influence of the airflow on water evaporation

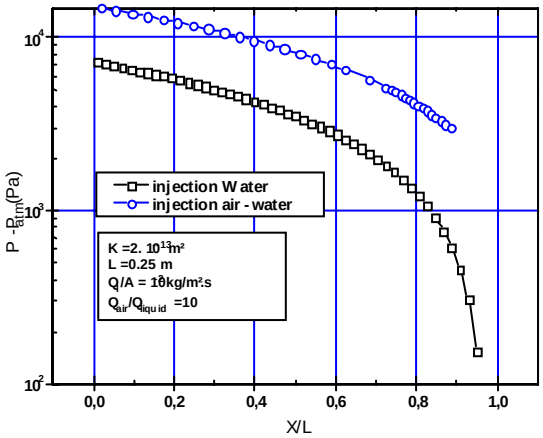

Figure 8. Influence of the airflow on water pressure of injection

6. CONCLUSION

1. In our study, we wanted to visualize the compression effect on the flashing liquid phenomenon. This effect is intimately related to the pressure drop. The energy equation adopted reveals this aspect while eliminating the other thermal aspects as convection, diffusion and source terms. The isentropic assumption allows to ignore the heat losses.

2. The averaging method applied to the energy equation in a representative elementary volume generates new terms related to the local fluctuations. Experiments in laboratories should predict the importance of these terms. Other experiments are necessary to realize in order to simulate a more a realistic conditions.

3. The liquid flow is described by a homogeneous multi-components model disregarding interactions between steam and the other phases (water and air). The calculated produced steam is negligible (x =10^{-4} to10^{-2}). If we consider a great production of steam carried out by heat contribution, it is therefore recommended to consider the separate flow model of the three phases: water/steam/air.

4. In general, we conclude that the flashing is influenced by the injected liquid mass flow rate, the length of the porous channel and the air mass flow rate, which represents an obstacle facing the water flow. This requires a sufficient pressure to ensure the water flow. This pressure moves away the liquid evaporation conditions toward the exit side.

REFERENCES

Carbonell R.G., Mutiphase flow models in packed beds, *Oil & gaz science and technology, vol. 55 N° pp. 417-425, rev. IFP, TECHNIP editions, 2000*

Chao-Yang Wang and Beckermann C., A two phase mixture model of liquid-gas flow and heat transfer in capillary porous media I- Formulation. *Int. J. Heat mass transfer vol.36, No.11, pp.2747-2758, 1993*

Fourar F. and Lenormand R. Inertial effect in two phase flow through fractures. *oil & gas science and technology, vol. 55 N° pp. 259-268, rev. IFP, TECHNIP editions, 2000*

Horne R.N, Satik C., Mahiya G., Li K.,.Ambusso W, Tovar R.,Wang C.and Nassori H., Steam-water relative permeabilty, *presented at the 2000 World geothermal Congress, Japan 2000.*

Houpert, A., Mécanique des fluides dans les milieux poreux critiques et recherches, *édition Technip, pp.185 220, 1974*

Institut Français du Pétrole, recherches et témoignages, l'exploitation des gisements d'hydrocarbures, domaines scientifiques et principes généraux, *Edition technip (1974)*

Kaviany M., Principals of heat transfer in porous media, *Mechanical engineering series*, Springer edition, 1995

Lackmé C., Thermodynamics of critical two-phase discharge from long pipe of initially subcooled water. *Nuclear reactor safety heat transfer. Dubrovnik (1980)*

Patankar, S.V., Numerical heat transfer and fluid flow, *Mac Graw Hill, 1980*

Seladji C., analyse du phénomène de flashing lors d'un écoulement diphasique dans un canal poreux, *presented at the mechanical congress : Morocco (2003)*